Numerical investigation of surface roughness effects on heat transfer in a turbine cascade

Cite as: AIP Conference Proceedings **2191**, 020143 (2019); https://doi.org/10.1063/1.5138876
Published Online: 17 December 2019

Arunprasath Subramanian, Andrea Gamannossi, Lorenzo Mazzei, et al.

Numerical Investigation of Surface Roughness Effects on Heat Transfer in a Turbine Cascade

Arunprasath Subramanian[1,a)], Andrea Gamannossi[2], Lorenzo Mazzei[3] and Antonio Andreini[3]

[1]*ISAE-ENSMA, Teleport 2, 1 Avenue Clement Ader, Chasseneuil-du-Poitou - 86360, France*
[2]*Department of Engineering and Architecture, University of Parma, Via Università 12, Parma - 43121, Italy*
[3]*Department of Industrial Engineering, University of Florence, Via S. Marta 3, Firenze - 50139, Italy*

[a)]Corresponding author: arunprasath.subramanian@ensma.fr

Abstract. Turbine entry temperature has seen a steady increase over the years as it is directly linked to the overall efficiency of a gas turbine engine, thus determining fuel consumption and ultimately CO_2 emissions. An accurate estimation of the heat loads is of paramount importance to design the cooling system and determine the life-span of the component, therefore it is mandatory to assess the capability of CFD to predict the involved phenomena. Surface roughness plays a key role in determining the heat transfer and becomes relevant especially in case of in-service degradation and additive-manufactured components. It is seen that for a turbine blade in service for about a thousand hours, the surface roughness has similar effects as turbulence on the heat transfer. This paper is focused on the study of the influence of roughness, turbulence and Reynolds number on the aerodynamics and heat transfer by using commercial code ANSYS Fluent. Transition was accounted exploiting the Transition-SST model, whereas roughness was modeled with an equivalent sand grain approach. Numerical results have been compared against experimental data from the literature.

INTRODUCTION

Gas turbines operating at higher temperatures have better efficiency and power output; however, achieving such improvements requires to address specific technological issues, such as the materials that cannot withstand the high gas temperature, which may cause enormous stress and eventual failure of the material [1]. Most materials have melting temperatures well below the gas temperature; therefore, their use is made possible only by the exploitation of cooling techniques and improved material properties. There has been an average increase of about 10 K in the turbine entry temperature every year and studies have shown that an increase of ≈ 56 K can improve the output by $8-13\%$ with an increase in cycle efficiency of $2-4\%$ [2].

Surface roughness is one of the most important factors affecting not only aerodynamics but also heat transfer and film cooling performance [3]. However, the difficulties associated to the experimental investigation as well as in including its effects in CFD simulations has hindered the development of extensive knowledge on the topic. Surface roughness of a turbine blade increases due to ash deposition and erosion due to high temperature and velocity of gases flowing through the turbine [4]. Recently, the interest in roughness effects has grown to the spread of additive manufactured components for gas turbine applications. This process in fact generates surface asperities with different behavioral properties than traditional manufacturing techniques. Therefore, it is even more important to qualitatively and quantitatively identify the effects of surface roughness on the convective heat loads of turbine blades.

Although extensive literature is available on surface roughness effects by experimental methods, there is little information on the characterization of surface roughness and the numerical modeling for additive manufactured components. The most common approach used in CFD consists using an equivalent sand grain roughness (ESGR), i.e. converting the real roughness in an equivalent layer of packed spheres. However, determining the correct input to be provided to the model is difficult, since the conversion from roughness parameters into the equivalent sand grain roughness height is affected by significant uncertainty [5].

74th ATI National Congress
AIP Conf. Proc. 2191, 020143-1–020143-10; https://doi.org/10.1063/1.5138876
Published by AIP Publishing. 978-0-7354-1938-4/$30.00

Equivalent sand grain roughness

The characteristics of the rough surface are usually described in terms of integral parameters like R_a, R_q, R_z and many others, used to describe shape, height, width of the asperities. Nevertheless, from a fluid dynamics point of view, experimentation on roughness was historically carried out using an "artificially created" roughness. Nikuradse [6] applied uniform sand grains to cover the pipe wall in which a new parameter called sand grain roughness height k_s was conceived. When flow in pipes is considered, the roughness of the wall is characterized by a single roughness parameter, the relative roughness k_s/R. Nikuradse's results are shown in Fig. 1 (a), variation of the friction factor with different Reynolds number is plotted. It is seen that for each value of R/k_s an individual friction factor curve is obtained. In the turbulent region of the flow each friction factor curve eventually tends to be constant as the Reynolds number increases [7].
In this region the friction factor is independent of the Reynolds number and is only a function of the relative roughness. This region, where the friction factor curves are constant, is a fully developed turbulent flow. For a turbulent flow, the friction factor λ can be written as follows [8]:

$$\frac{1}{\sqrt{\lambda}} = 2log\frac{R}{K_s} + 1.74 \tag{1}$$

The roughness density parameter defines how densely the roughness elements are packed on the surface. It is an important parameter which takes into account the total frontal area, the wetted surface area, surface area of the roughness element. It is defined by Van Rij et al. [9] as:

$$\Lambda_R = \frac{A_s}{A_f}\left(\frac{A_f}{A_w}\right)^{1.6} \tag{2}$$

Laminar-to-turbulent transition

One of the major factors that augment the heat transfer into a blade in the laminar-turbulent transition. The transition process is heavily dependent on the Reynolds number. The flow remains laminar up to certain Reynolds numbers and once the threshold is reached it is possible to observe a transitional phase which leads to turbulent flow through various physical mechanisms.

It is believed that the minute disturbances in the flow translate into two dimensional waves which tend to expand into the span wise direction giving rise to a complex three dimensional phenomena [10]. The transition process starts with a stable laminar flow near the leading edge leading to 2-D Tollmien-Schlitchting waves. These waves give rise to unstable 3-D waves and horse shoe vortices. These vortices break down in the regions of high shear leading to a series of vortex break downs into disturbances in all three directions. These lead to the formation of turbulent spots at areas where there are high velocity fluctuations which combine to form a fully turbulent flow [11].

The effect of wall roughness on the transition is a complex phenomenon. It is seen that if the roughness elements are smaller than the displacement boundary layer thickness δ, there is little effect due to the roughness element, but as the roughness height increases, the effect of roughness starts to play a major role in transition onset as well as modifying the thickness of the momentum and displacement boundary layer thickness. In general, presence of roughness elements fastens the transition and this effect further amplifies with increase in the Reynolds number[12]. In this article the effect of the free stream turbulence, wall roughness and the Reynolds Number of the flow on the transition and subsequently the heat transfer into the turbine blade are studied.

Investigated test case

Various experiments on a roughened heavily-loaded gas turbine blade were conducted in Karlsruhe at the Institute of Thermal Turbomachinery (KIT) [13, 14, 15] and by Lorenz et al. [16, 17] to quantify the effects of surface roughness. As shown in Fig. 1(b), they used a linear cascade with an electric heater so as to heat the mainstream. The temperature was measured with thermocouples at regular intervals to have a good accuracy of the temperature and heat flux distribution over the blade. In order to evaluate the impact of mainstream turbulence on the blade, different grids and different distances from the leading edge were tested and compared to a case in absence of any grid. Additional information about the turbulence generation and the resulting turbulence quantities to be applied at the inlet of the computational domain are described later on in Table 3. As far as the roughness effects is concerned, rough metal foils

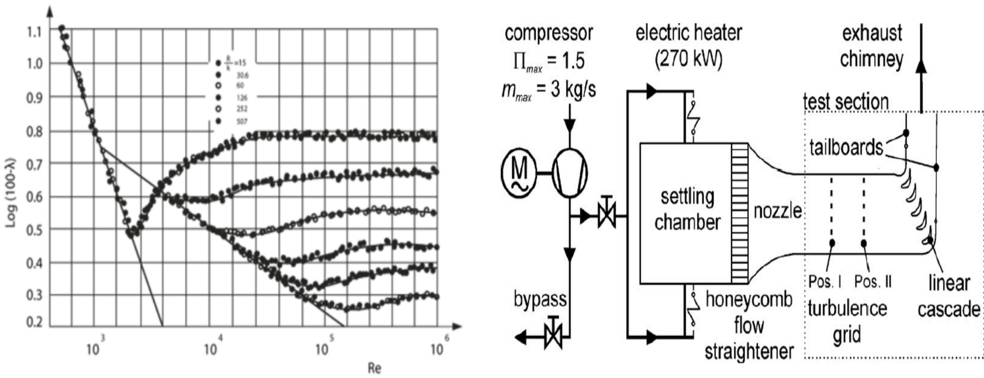

FIGURE 1: (a) Friction factor data of Nikuradse for artificially roughened pipes and (b) schematic representation of the test case with various dimensions (adapted from Lorenz et al. [16])

with elliptic pimples were used to recreate surface roughness in the experimental case. For the numerical investigation , the equivalent sand grain roughness using the method of Van Rij et al. is adapted [9] . Each of the roughness case was tested for every Reynolds number case and every turbulence intensity tested.

Numerical setup

The geometry of the blade was created using CATIA v5 and the modelled geometry is shown in Fig. 2. The coordinates of the profile were obtained from the thesis report of Lorenz [18]. Since the test case consists of a linear cascade and considering that secondary flows should not affect the midspan region where the measurements were performed, the problem can be approximated to be two dimensional. The domain is shown in the Fig. 2, with specifications of the boundary conditions. As it is possible to notice, the computational grid was 2.5D, i.e. consisting of only one extruded element in radial direction. The mesh statistics are shown in Table 1. In order to get a good resolution of the leading edge and the trailing edge where the hotspots are predominant, a mesh refinement was applied. A prismatic layer mesh with 30 layers were used to capture the boundary layer accurately and provide a y^+ well below 1 for the smooth cases. The results obtained $k - \omega$ SST and Transition-SST [19] models are reported in Fig. 4 (b). It is clearly observable

TABLE 1: Mesh configurations with cell statistics

Mesh type	Cells	Max cell size	Face sizing
2.5D	60,000	1.5 mm	1.5 mm
2.5D	85,000	1.5 mm	1 mm
2.5D	150,000	1.5 mm	0.5 mm (w/o leading edge refinement)
2.5D	200,000	1.5 mm	0.5 mm (w/ leading edge refinement)

that the Transition-SST performs the best due to the relevance of transition for this test case. While the $k - \omega$ SST reproduces a fully turbulent behaviour immediately downstream of the leading edge, accounting properly for the transitional behaviour of boundary layer allows to keep the laminar nature along most of the suction side, coherently with the experimental data. A minor mismatch appears on the pressure side, where the transition is slightly anticipated. This aspect will be addressed in more details when the impact of turbulence level will be discussed.

Boundary conditions

Concerning the boundary conditions, the value of velocity at the inlet was calculated so as to match the Reynolds numbers of 50000, 150000 and 250000, which were calculated using the chord $c = 65.23\ mm$ as characteristic length, a density of 1.04 kg/m^3 and a dynamic viscosity of $2.074e - 5\ kg/ms$. The inlet angle was specified at 27° and inlet total temperature as 350 K as in the experimental test case. A constant temperature value of 300 K was applied to

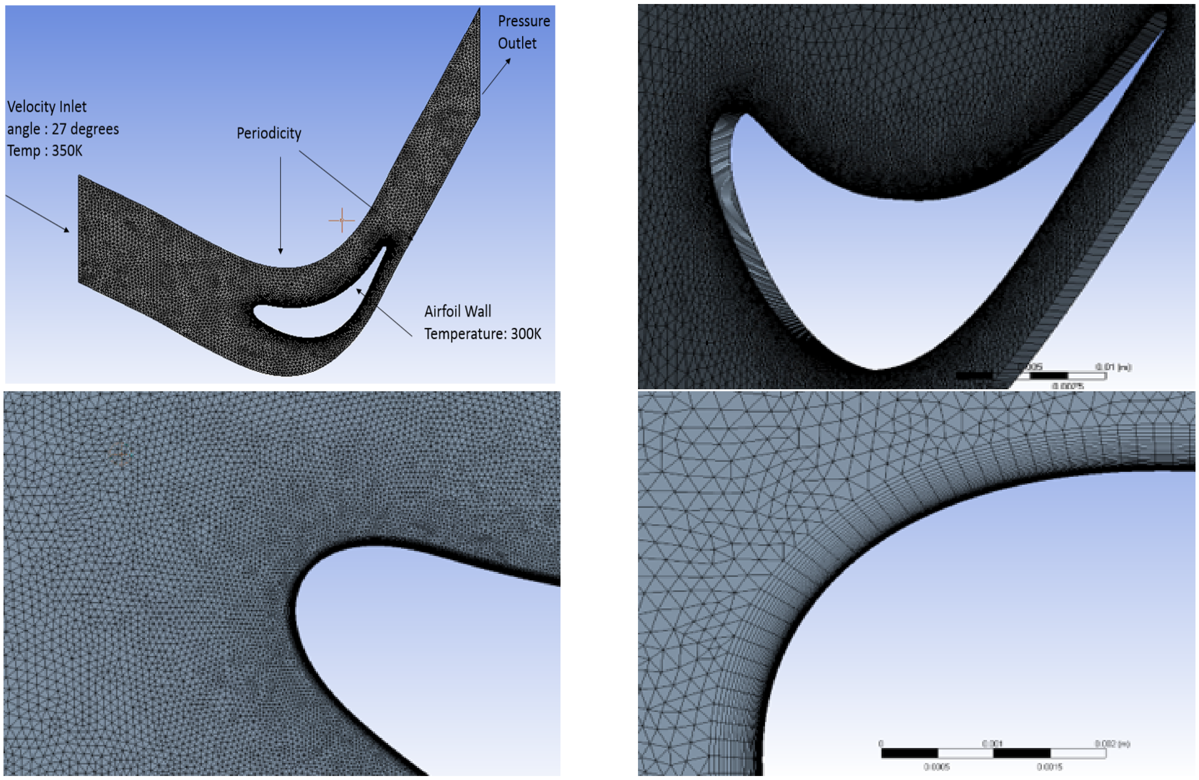

FIGURE 2: Details of the computational domain, boundary conditions and mesh.

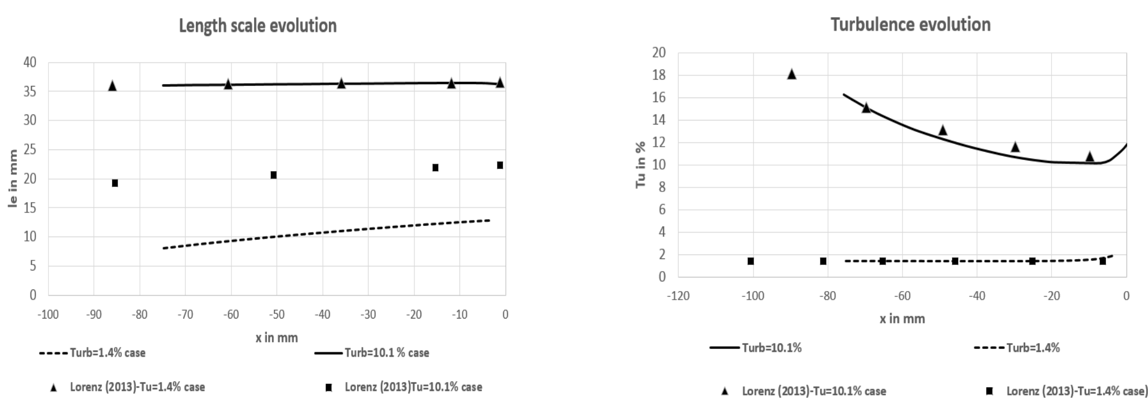

FIGURE 3: Turbulence and length scale evolution for current cases(lines) and experimental observations [18]

the blade.The reference pressure is set as 1 bar. An iterative procedure was used to determine the back pressure at the outlet in order to match the right values of inlet total pressure. The boundary conditions are summarized in Table 2. Estimating the most appropriate set of turbulence quantities to be applied at the inlet was not a straightforward task, as the experimental activity reported turbulence intensity Tu and length scale L generated by the grids and measured just upstream on the blade leading edge. Therefore, an iterative procedure was performed to obtain the set of turbulence quantities to be applied at the inlet of the domain so as to match the values at the leading edge and a representative turbulence decay.The final set applied at the inlet is specified in Table 3 with particular reference to the turbulence intensity Tu_{in} and the length scale L_{in}.A good evolution in terms of turbulence intensity but a mismatch in the evolution of the length scale is observed as seen in Fig. 3

TABLE 2: Boundary conditions

Boundary condition	Type	Value		
Inlet	Velocity [m/s]	16.25	48.32	76.11
	Re	50,000	150,000	250,000
	Total temperature [K]	350	350	350
Outlet	Static pressure outlet [Pa]	99900	97900	96790
Wall	Temperature [K]	350	350	350

TABLE 3: Turbulence quantities applied to the inlet depending on the grid configurations.(Tu_{grid} and l_{grid} values are experimentally observed values whereas Tu_{in} and l_{in} represent the values specified at the inlet)

Grid	Tu_{grid} [%]	l_{grid} [mm]	Tu_{in} [%]	l_{in} [mm]
-	1.4	37	1.42	8
1	4.2	7.8	7.2	12
2	7	22.4	9	32
3	10.1	16.5	16.4	36

Results and discussion

Isentropic Mach number

The discussion of the results starts focusing on the isentropic Mach number distributions, calculated for Reynolds number varying between 50,000 and 250,000. The isentropic Mach number is calculated according to the expression:

$$Ma_{is} = \sqrt{\left(\frac{2}{\gamma - 1}\right)\left[\left(\frac{P_s}{P_{t,in}}\right)^{\frac{1-\gamma}{\gamma}} - 1\right]}$$

The values were compared against those of the experimental test cases in terms of Ma_{is} against S/C, the abscissa normalized by the blade chord: looking at Figure 4(a) it can be noticed that there is high conformity on both pressure ($S/C < 0$) and suction side ($S/C > 0$). The maximum value of isentropic Mach is observed at about 70% of the chord, as expected from an aft loaded gas turbine blade.

Turbulence

From Figures 5(a)-5(d) it is possible to notice that the variation in the turbulence level has a direct effect on the heat transfer. An increase in the turbulence intensity causes the Nusselt number to increase due to enhanced mixing between the freestream and the boundary layer, leading to higher heat flux into the wall.

For the lowest turbulence intensity case, as already shown in Figure 4, on the suction side the Nusselt number matches the experimental values, although on the pressure side the peak where the transition occurs is anticipated

TABLE 4: Roughness cases investigated [16]

Case	$k_{s,Rij}$ [9]
Smooth	Hydraulically Smooth
r20a	31.9
r40a	69.6
r80a	147

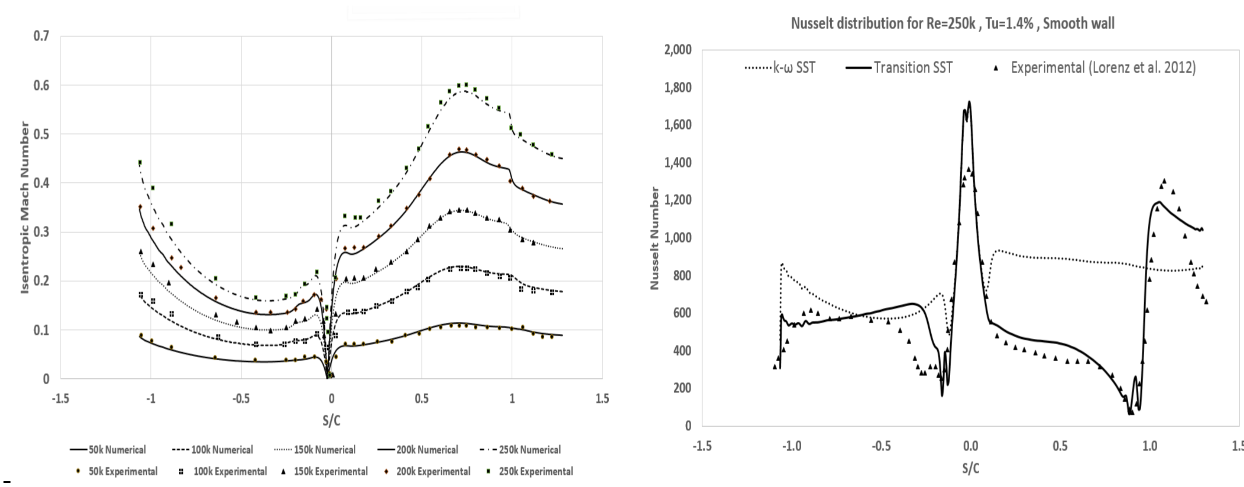

FIGURE 4: (a) Isentropic Mach number distribution for Re between 50,000 and 250,000. (b) Nusselt number distribution :Comparison of $k - \omega$ SST and Transition-SST with the experimental results

and overestimated. Interestingly, this peak becomes observable also in the experiments at higher turbulence intensity, showing a sensitivity that the CFD model is not capable of reproducing at low Tu values.

Overall, as the turbulence intensity increases, there is a general overestimation of the Nusselt number and an earlier transition from laminar to turbulent flow. However, the results on the suction side are well predicted and in accordance with experimental results, probably suggesting that additional verification on the actual turbulence level and its decay would be necessary.

Roughness

So far, we have seen results for the smooth cases with no added roughness elements. As described earlier, we will use three roughness cases r20a, r40a, r80a and compare them with experimental results. For the lowest Reynolds number case, it can be observed that adding roughness elements has no impact on the Nusselt number distribution (see Figure 6) as observed in the experimental results [16].

For the high turbulence intensity case with 10.1% a slightly higher Nusselt number is reported and the transition happens more smoothly compared to the lowest turbulence intensity case and results are comparable to the expected results from experiments. One can therefore conclude that the Transition SST model predicts the heat transfer accurately at low Reynolds numbers, irrespective of the turbulence intensity or roughness elements.

Moving on to higher Reynolds number at $Re = 150,000$ (Figure 7 left), significant changes for the low turbulence intensity $Tu = 1.4\%$ case are observed. A general increase in the heat transfer into the blade can be observed and ascribed to the increase in Reynolds number. As already observed, the smooth case i always predicted fairly well by CFD. Once roughness is included, it is seen that a slight over-prediction progressively arises on the pressure side with increasing roughness levels (cases r20a and r40a). For the very high roughness case (r80a) the simulation underpredicts the Nusselt distribution and the pressure side transition onset location is completely missed.

For the high Reynolds number case of $Re = 250,000$ (Figure 7 right), similar conclusions can be drawn, except that at this condition the transition onset is clearly triggered earlier. Already for the r40a case the transition takes place in a smoother way, whereas for maximum roughness it occurs just downstream of the leading edge. The CFD partly succeeds in reproducing this effect, with a transition too much anticipated in an early stage (r40a case) and not sensitive enough for high roughness conditions (r80a case). Indeed the highest roughness conditions, at least for low Tu values, seems the most detrimental for CFD, with an unclear tendency to reduce the Nusselt number on the leading edge, which seems in contrast with the experimental evidences.

For the cases at high turbulence intensity and medium Reynolds number (Figure 8 left)significant changes compared to the low turbulence intensity $Tu = 1.4\%$ case are observed. As expected it is possible to observe a general increase in the heat transfer on the blade. For the smooth case there is an over prediction of about 10% on both suction and pressure side for the Nusselt number. Adding a small roughness value, there is a high over prediction on the

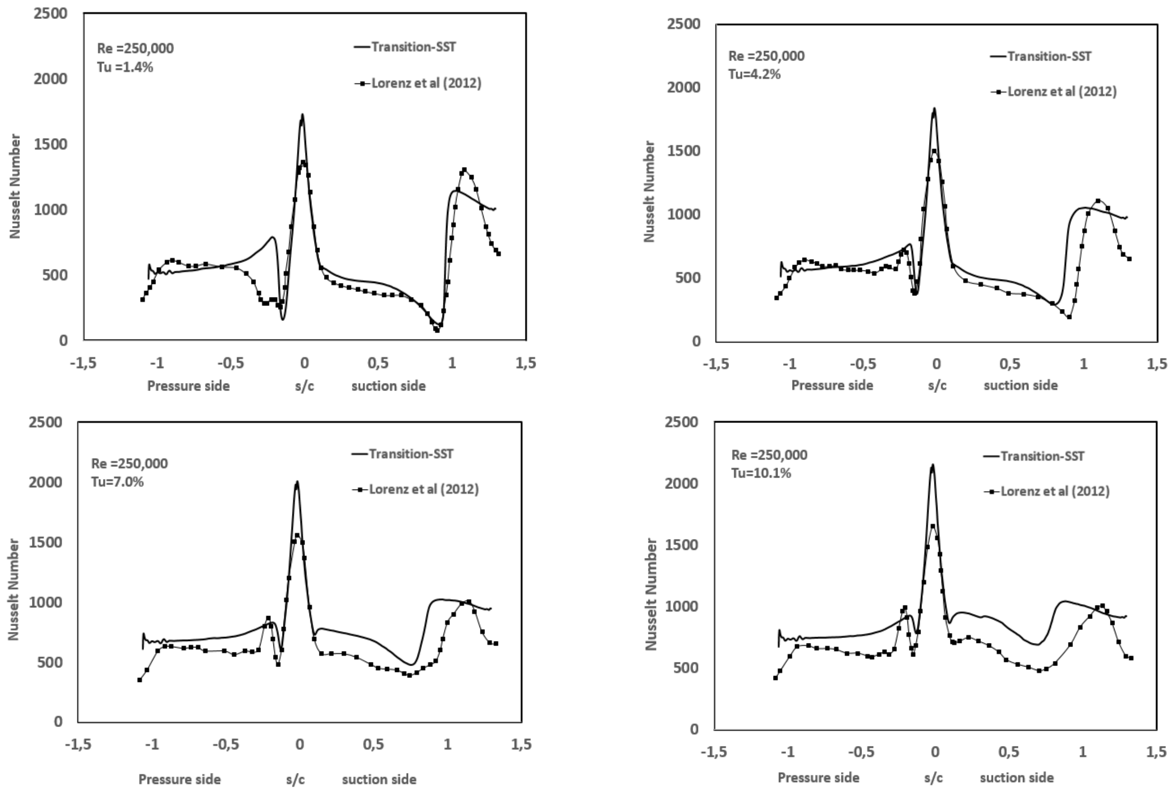

FIGURE 5: Nusselt number distributions at different turbulence intensity (Re = 250, 000, smooth wall).

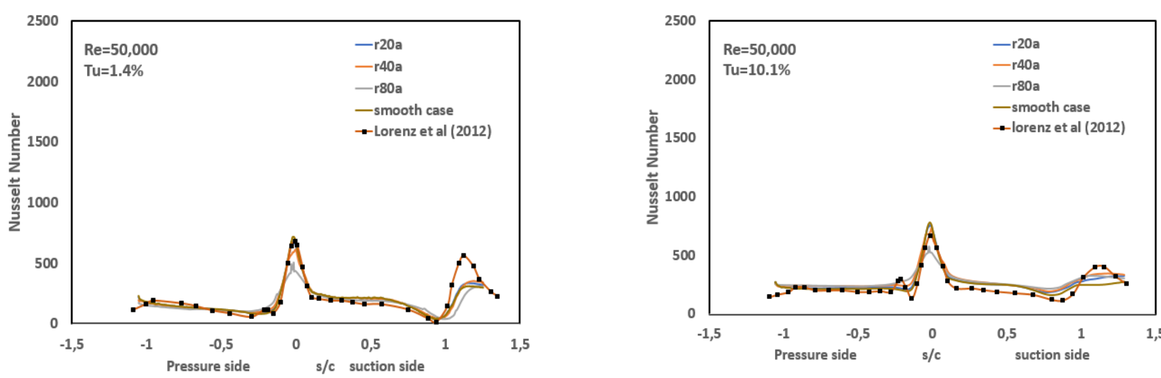

FIGURE 6: Nusselt distributions for various roughness cases at low Reynolds number (Tu = 1.4%) in comparison with experimental results from Lorenz.(Only one curve from experiment is shown so as to eliminate cluttering)

suction side and the transition occurs significantly earlier than expected. A further increase in the roughness yields no better results and the model still predicts a too sudden transition from a laminar to turbulent flow. For the highest Reynolds number case (Figure 8 right), there is an over prediction on the suction side, but with a slightly earlier transition predicted at about 0.9c. The introduction of a small roughness drastically increases the heat flux into the blade and this is seen from the Nusselt distribution. Similarly for higher roughness cases, the order of magnitude of the results match fairly well but the peaks are slightly misaligned from the values obtained from the experimental results.

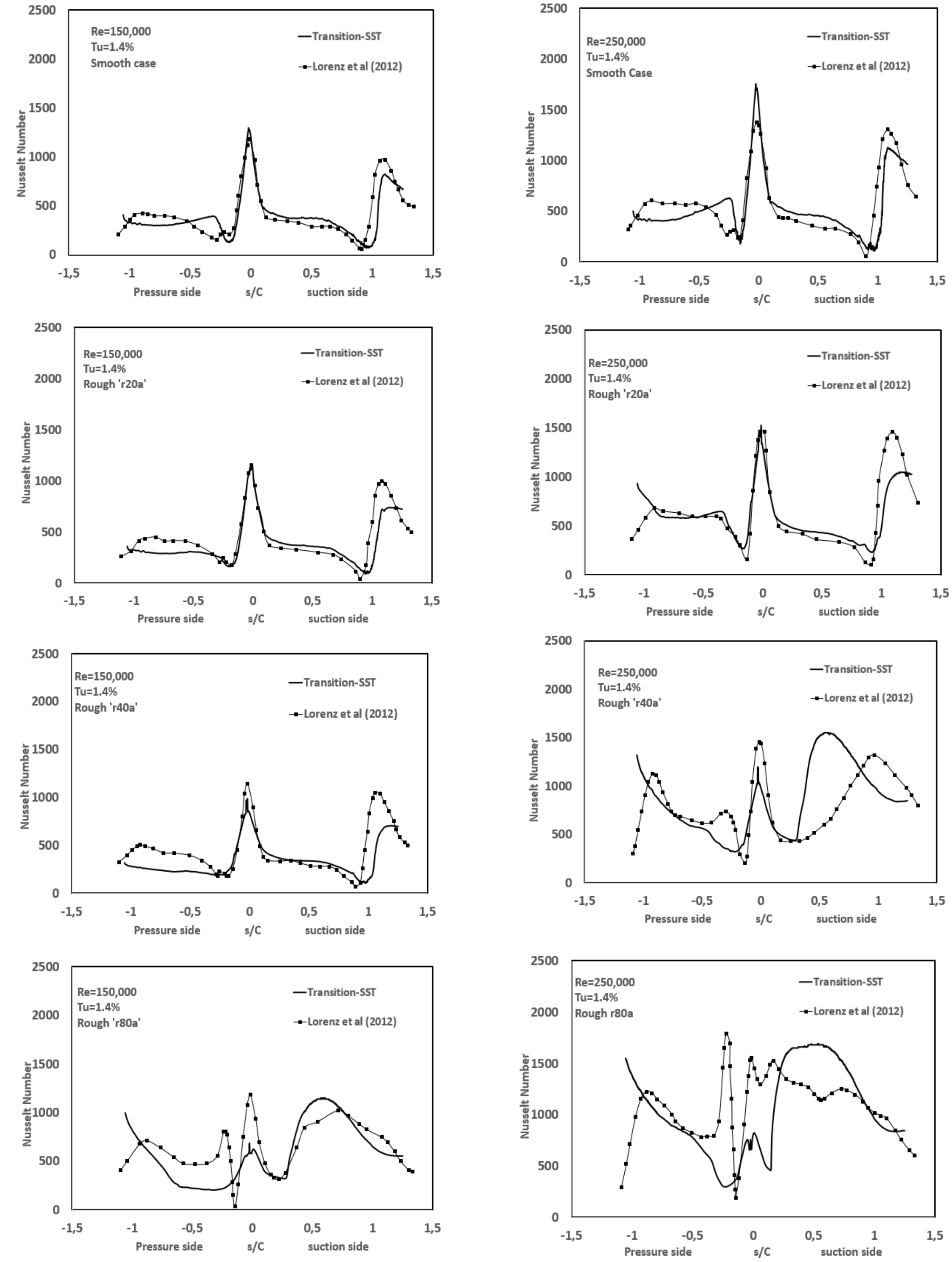

FIGURE 7: Nusselt distributions for various roughness cases at medium and high Reynolds number (Tu = 1.4%).

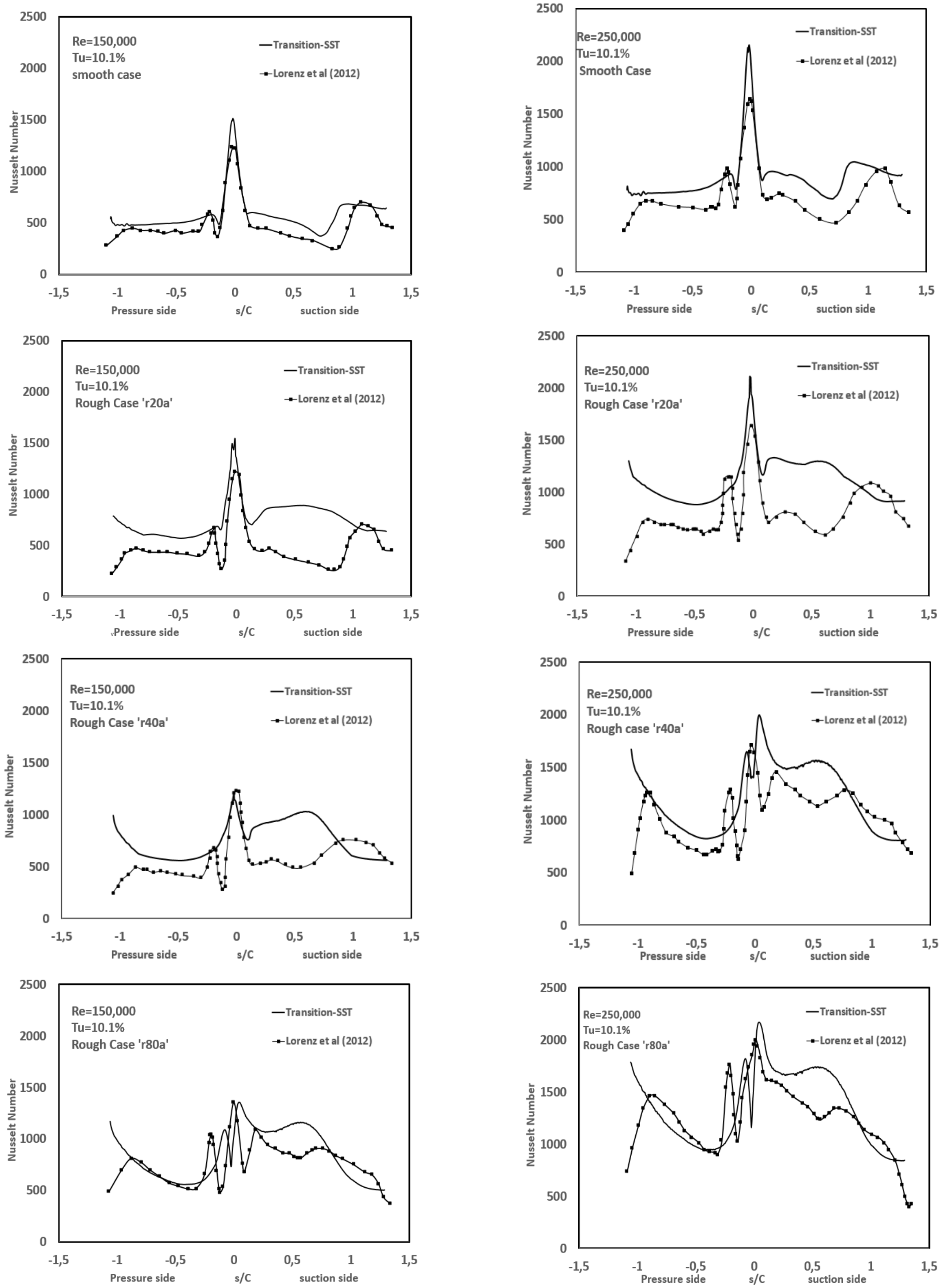

FIGURE 8: Nusselt distributions for various roughness cases at medium and high Reynolds number (Tu = 10.1%).

Conclusions

The capability of CFD to reproduce the impact of Reynolds number, turbulence level and surface roughness on the heat transfer was investigated in this work. The Transition-SST model was used to address the presence of boundary layer transition on the airfoil. The benchmark performed against dedicated experimental data showed that the proposed numerical setup succeeds in simulating accurately the Nusselt number distribution, even though it appears too sensitive to the increase in turbulence intensity compared to the experimental evidences.

From an experimental point of view the roughness plays a more relevant role when the Reynolds number is increased, indicating that the boundary layer is progresses from an hydraulically smooth to a transitionally rough and a fully rough condition. Under these circumstances, the good performance achieved by CFD with smooth wall conditions are progressively degraded, which translates into a mismatch in the transition onset and overall magnitude of the heat transfer level. Possible explanations of this phenomenon can be attributed to:

- Wrong turbulence level assigned and/or misprediction in the turbulence decay
- Uncertainty associated to the estimation of the equivalent sand-grain roughness k_s imposed to the airfoil
- Inaccurate behaviour of the Transition-SST model with particular reference to its sensitization to the wall roughness

In order to clarify these aspects, more efforts should be devoted to better investigating the characteristics of turbulence, testing the sensitivity of the results to the estimated value of k_s as well as the capability of different transition models to account for wall roughness.

REFERENCES

[1] H. Cohen and F. J. Bayley, "Heat-transfer problems of liquid-cooled gas-turbine blades," (SAGE Publications, 1955), pp. 1063–1080.

[2] M. P. Boyce, *Gas turbine engineering handbook* (Elsevier, 2011).

[3] J.-C. Han, S. Dutta, and S. Ekkad, *Gas turbine heat transfer and cooling technology* (CRC Press, 2012).

[4] D. N. Barlow and Y. W. Kim, "Effect of surface roughness on local heat transfer and film cooling effectiveness," in *ASME 1995 International Gas Turbine and Aeroengine Congress and Exposition* (American Society of Mechanical Engineers, 1995), pp. V004T09A014–V004T09A014.

[5] J. P. Bons, "A review of surface roughness effects in gas turbines," (American Society of Mechanical Engineers, 2010) p. 021004.

[6] J. Nikuradse, "Forschung auf dem gebiete des ingenieurwesens," (1933) p. 361.

[7] E. Bobok, *Fluid Mechanics for Petroleum Engineers* (Elsevier S&T, 1993).

[8] J. Nikuradse, *Laws of flow in rough pipes* (National Advisory Committee for Aeronautics Washington, DC, 1950).

[9] J. A. Van Rij, B. Belnap, and P. Ligrani, Journal of fluids engineering **124**, 671–677 (2002).

[10] E. Ghasemi, D. McEligot, K. Nolan, J. Crepeau, A. Siahpush, R. Budwig, and A. Tokuhiro, International Journal of Heat and Mass Transfer **77**, 475–488oct (2014).

[11] D. S. H. Peter J. Schmid, *Stability and Transition in Shear Flows* (Springer New York, 2012).

[12] N. R. Vadlamani, P. G. Tucker, and P. Durbin, "Distributed roughness effects on transitional and turbulent boundary layers," (Springer Nature, 2017), pp. 627–649.

[13] M. Stripf, A. Schulz, and S. Wittig, *ASME Turbo Expo 2004: Power for Land, Sea, and Air*, 1–10 (2004).

[14] M. Stripf, A. Schulz, and H. Bauer, "Surface roughness and secondary flow effects on external heat transfer of a high pressure turbine vane," in *17th International Symposium on Airbreathing Engines, Sept* (2005), pp. 4–9.

[15] M. Stripf, A. Schulz, H.-J. Bauer, and S. Wittig, Journal of Turbomachinery **131**, p. 031016 (2009).

[16] M. Lorenz, A. Schulz, and H.-J. Bauer, J Turbomach. **134**, p. 041006 (2012).

[17] M. Lorenz, A. Schulz, and H.-J. Bauer, J Turbomach. **134**, p. 041007 (2012).

[18] M. V. Lorenz, "Einfluss der Oberflächenrauigkeit auf den Wärmeübergang und die aerodynamischen Verluste einer Gasturbinenbeschaufelung: experimentelle Untersuchungen und Entwicklung einer Korrelation für den laminar-turbulenten Umschlag," Ph.D. thesis, Karlsruher Institut fr Technologie (KIT) 2013.

[19] F. R. Menter, R. Langtry, and S. Vlker, Flow, Turbulence and Combustion **77**, 277–303aug (2006).